Modelling the Time-Course of the Tissue Responses to Intramuscular Long-Acting Paliperidone Palmitate Nano-/Microcrystals and Polystyrene Microspheres in the Rat

Nicolas Darville[1,3*], Marjolein van Heerden[2*], Tim Erkens[2], Sandra De Jonghe[2], An Vynckier[2], Marc De Meulder[2], An Vermeulen[3], Patrick Sterkens[2], Pieter Annaert[1], and Guy Van den Mooter[1]

[1]*Drug Delivery and Disposition, Department of Pharmaceutical and Pharmacological Sciences, KU Leuven – University of Leuven, Leuven, Belgium*

[2]*Preclinical Development and Safety, Janssen Research & Development, a Division of Janssen Pharmaceutica NV, Beerse, Belgium*

[3]*Model Based Drug Development, Janssen Research & Development, a Division of Janssen Pharmaceutica NV, Beerse, Belgium*

[*]*Both Nicolas Darville and Marjolein van Heerden contributed equally to the article.*

SUPPLEMENTAL MATERIAL AND METHODS

Semi-Quantitative Histopathology

Table S-1. Semi-quantitative histopathology parameters evaluated on a scale from 0 to 5 for each animal of the PP-LAI and PS test groups.

Parameter	Definition and comments
Inflammation	General degree of inflammation, composite parameter reflecting the extent of the local tissue response (*i.e.* oedema, vascular activation, extravasation and/or infiltration of acute and/or chronic inflammatory cells, angiogenesis and fibrosis); assessed on H&E sections
Oedema	Interstitial fluid (eosinophilic, protein-rich) in endo-, peri- or epimysium; assessed on H&E sections
Myofibre de-/regeneration	Degeneration: vacuolated myofibres with hyalinized stroma, eosinophilic sarcoplasm and loss of striation, or sarcolemma disruption. Regeneration: proliferation of satellite cells, small diameter myofibres with internal nuclei and basophilic sarcoplasm or reduced striations; both assessed on H&E sections
Depot cellularization:	Extent of the cellular infiltration and cellularity within the formulation depot; as the granulocyte/macrophage infiltration is a centripetal process, the scores are also representative of the infiltration depth relative to the observed depot dimensions
Granulocyte infiltration	Extent of infiltration of granulocytes (mainly neutrophils) within the formulation depot/granulation tissue; assessed on H&E sections
Macrophage infiltration	Extent of infiltration of macrophages within the formulation depot/granulation tissue; assessed on CD68 sections
T cell infiltration	Prevalence of T lymphocytes within the formulation depot/granulation tissue; assessed on CD3-ε sections
B cell infiltration	Prevalence of B lymphocytes within the formulation depot/granulation tissue; assessed on CD79b sections

Granulation tissue	Continuous layer of macrophages, in combination with fibroblasts, collagen and T cells at later time points, surrounding or replacing the entirety of the formulation depot; scoring: “absent” or “present”; assessed on H&E sections
Angiogenesis	Extent of neovascularization (*i.e.* infiltrating capillaries) in the formulation depot/granulation tissue; assessed on CD31 sections
Phagocytic macrophages	Estimated degree of formulation/foreign particulate material within swollen macrophages, compared to the remaining formulation depot; assessed on H&E and CD68 sections
Giant cells	Presence of multinucleated giant cells (MNGC); assessed on H&E and CD68 sections

Quantification of the Depot Geometry and Cellularization

The circularity (*C*) of the polygonal selection was measured as an indication of the depot geometry and is a function of the cross-sectional depot area (S_{depot}) and the depot perimeter (P_{depot}) (Equation S-1). A value equal to unity implicates perfect sphericity, while values approaching 0 indicate increasingly elongated or irregular shapes.

$$C = 4\pi \cdot S_{depot} / {P_{depot}}^2$$

…….....Eq. S-1

Quantification of the Depot Vascularization

Similar to the processing of H&E sections, adjacent CD31-stained sections were scaled, the contour of the formulation depot was defined and S_{depot} was measured. Colour, brightness and/or contrast thresholding was applied to the already contrasted immunohistological RGB image to create a selective mask for positively stained structures. The selection (*i.e.* vascular tissue within the contour of the formulation depot) was converted to a binary image, the edge finding algorithm was applied and the total cross-sectional area of the $CD31^+$ vascular structures was measured using the particle counting function in ImageJ. The extent of the angiogenesis was expressed as the fraction of the area relative to S_{depot}, as a function of time. Results are presented as mean values ± SD (n = 3).

Derivation of Formula for the Fraction Volume Infiltrated by Inflammatory Cells

An ellipse with major axis A and minor axis *B* has an aspect ratio *R*, given by Equation S-2.

$$R = \frac{A}{B}$$

……...……Eq. S-2

The surface area of an ellipse ($S_{ellipse}$) with major axis *A*, minor axis *B* and aspect ratio *R*, is given by Equation S-3.

$$S_{ellipse} = \frac{1}{4} * \pi * A * B$$

……...…….……...Eq. S-3

Substitution of *B* with *A/R* in Equation S-3 yields Equation S-4.

$$S_{ellipse} = \frac{1}{4} * \pi * \frac{A^2}{R}$$

……...…….……...Eq. S-4

The revolution of an ellipse with major axis *A* and minor axis *B* along its major axis yields a prolate spheroid with volume $V_{prolate}$ (Equation S-5), polar axis *A* and equatorial axis *B*.

$$V_{prolate} = \frac{1}{6} * \pi * A * B^2$$

…….……..Eq. S-5

Substitution of *B* with *A/R* in Equation S-5 yields Equation S-6.

$$V_{prolate} = \frac{1}{6} * \pi * \frac{A^3}{R^2}$$

…….……..Eq. S-6

Simple isolation of *A* in Equation S-4 and substitution for *A* in Equation S-6 yields an expression for $V_{prolate}$ as a function of $S_{ellipse}$ and *R* (Equation S-7).

$$V_{prolate} = \frac{4}{3} * \frac{{S_{ellipse}}^{3/2}}{\sqrt{\pi * R}}$$

……..……..Eq. S-7

Consider the surface area of the best fit ellipse to the cross-section of the depot (S_{depot}, Figure S-1a) that is characterized by a major axis *A*, minor axis *B* and aspect ratio *R*. Consider then the surface area of the best fit ellipse to the residual, un-infiltrated portion of the depot ($S_{resid.}$; Figure S-1a) that is characterized by a major axis *A'* and minor axis *B'*, with *A'*< *A* and *B'*< *B*. In analogy to the above, the revolution of these ellipses along their respective major axes creates prolate volumes for the depot (V_{depot}) and for the residual, un-infiltrated portion of the depot ($V_{resid.}$). The volume fraction that remains un-infiltrated ($F_{Vresid.}$) is then given by the ratio of $V_{resid.}$ to V_{depot} (Equation S-8).

$$F_{V_{resid.}} = \frac{V_{resid.}}{V_{depot}} = \frac{\left(\frac{4}{3} * \frac{{S_{resid.}}^{\frac{3}{2}}}{\sqrt{\pi * R'}}\right)}{\left(\frac{4}{3} * \frac{{S_{depot}}^{\frac{3}{2}}}{\sqrt{\pi * R}}\right)}$$

……..……..Eq. S-8

If the depot infiltration is assumed to be a symmetric and concentric process, then *R'* = *R*. $F_{Vresid.}$ can then be rewritten as an exponent of the fraction of the cross-sectional depot area that remains un-infiltrated ($F_{Sresid.}$), which is obtained by experimental measurement of the total cross-sectional area of the depot (S_{depot}) and the area of the residual, un-infiltrated portion of the depot ($S_{resid.}$) (Equation S-9).

$$F_{V_{resid.}} = \left(\frac{S_{resid.}}{S_{depot}}\right)^{\frac{3}{2}} = {F_{S_{resid.}}}^{\frac{3}{2}}$$

……..……..Eq. S-9

It follows from the definition of $F_{SAresid.}$ that it represents the difference between unity and the fraction of the cross-sectional depot area that has been infiltrated ($F_{Sinfiltr.}$) (Equation S-10).

$$F_{S_{resid.}} = 1 - F_{S_{infiltr.}}$$

……..……..Eq. S-10

Analogously, the volume fraction that has been infiltrated ($F_{Vinfiltr.}$; *i.e.* the volume of the outer layer depot that has been infiltrated) is given by Equation S-11.

$$F_{V_{infiltr.}} = 1 - F_{V_{resid.}}$$

……....….Eq. S-11

Substitution of Equation S-10 and Equation S-11 for $F_{Sresid.}$ in Equation S-9 yields the final expression for $F_{Vinfiltr.}$ (Equation S-12).

$$F_{V_{infiltr.}} = 1 - (1 - F_{S_{infiltr.}})^{3/2}$$

……..……Eq. S-12

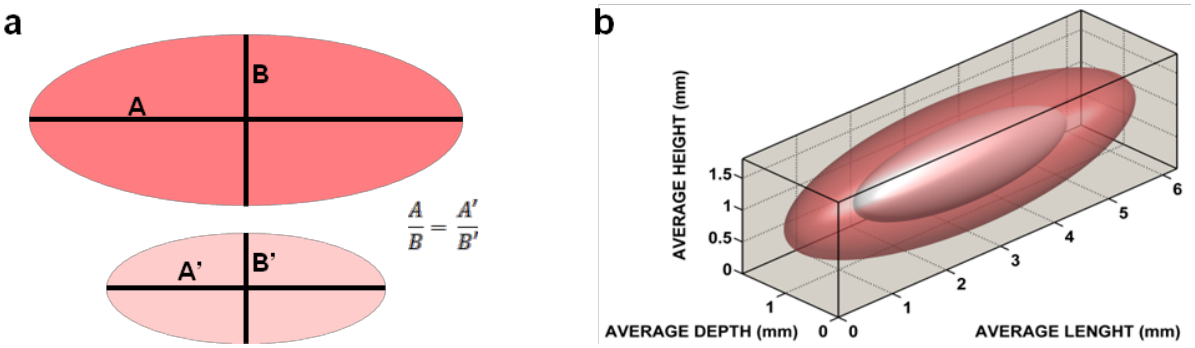

Figure S-1. Schematic representation of PP-LAI or PS im depot sagittal cross-sections. **a**) Ellipses representing the total cross-sectional depot area (S_{depot}; top) and representing the cross-sectional area of the residual, un-filtrated portion of the depot ($S_{resid.}$; bottom), characterized by major axes *A* and *A'*, and minor axes *B* and *B'*, respectively. **b**) Three-dimensional representation of the total depot volume (outer, dark) and the residual/un-infiltrated prolate volume (inner, light), assuming symmetry along the major axis of a sagittal cross-section of the depot.

Modelling the Depot Infiltration

The secondary model parameter $T_{50\%}$, represents the time at which half of the depot (either in terms of its cross-sectional area or as its extrapolated volume) has been infiltrated by cells. $T_{50\%}$ was derived from the value of α (Equation S-13).

$$T_{50\%} = (-\ln(0.5) \cdot \alpha)^{1/\beta} + T_0$$

.....Eq. S-13

Quantification of PP and PAL in Draining Lymph Nodes

The frozen lymph nodes were thawed at ambient temperature prior to homogenization in approximately 9 parts of water. 50 µl of the homogenized samples were transferred to a 96-well microplate. 100 µl of methanol was added to each well prior to vortexing for 3 min. 50 µl of a combined internal standard dilution (JNJ-3905343 for PP and JNJ-17340362 for PAL, 2.00 ng each/100 µl methanol) were added to the previous mixture and the plates were vortexed for 3 min. 200 µl of acetonitrile was supplemented to each well prior to vortexing for 3 min and centrifugation at ambient temperature for 10 min at 6000 × *g*. PAL was quantified in the undiluted supernatant. For the analysis of PP, 100 µl supernatant aliquots were added to 50 µl of tetrahydrofuran (THF) in another plate with subsequent vortexing.

Calibration and quality control samples were prepared by spiking PP/PAL dilutions (5–2500 ng/ml in methanol) to 100 µl of 50:50 *v/v* blank lymph node homogenate:methanol mixture prior to further sample preparation as described above. Calibration curves for PP and PAL were obtained by least squares linear regression of the log-transformed peak area ratios of PP:JNJ-3905343 and PAL:JNJ-17340362, respectively, against the log-transformed PP or PAL standard concentrations. The LLOQ (signal:noise ratio ≥ 5 with %CV ≤ 20% and mean accuracy within 80–120% of nominal value) for PP and PAL were 4.00 and 5.00 ng/g lymph node, respectively.

Quantification of PP and PAL in the supernatant was performed by means of high performance liquid chromatography with tandem mass spectrometric detection on a Shimadzu system consisting of LC-20 pumps, a mobile phase degasser and a SIL-HTc autosampler set at 4°C (Shimadzu Corp., Tokyo, Japan). Sample volumes of 10 µl were injected onto a 30 × 4.6 mm (5 µm particle size) Polaris® C18-A column (Varian Inc., Palo Alto, CA, USA). For PP and JNJ-3905343, the mobile phase constituents were: (A) 0.01 M ammonium acetate, (B) 0.01 M ammonium acetate in methanol/acetonitrile (33:67 *v/v*) and (C) THF. The chromatographic

separation was performed by isocratic elution with 17/50/33 A/B/C (*v/v/v*) for 0.5 min with subsequent 0.35 min step gradient with 2/50/48 A/B/C (*v/v/v*) and re-equilibration prior to the next injection. The flow rate was 2.5 ml/min with a 1.0 ml/min split directed to an API 4000® triple quadrupole mass spectrometer equipped with a Turbo-Ionspray® ionization source (AB Sciex Inc., Framingham, MA, USA). The total run time was 1.5 min and the retention times for PP/JNJ-3905343 and PAL/JNJ-17340362 were 0.46 and 0.49 min, respectively. The mass spectrometer was operated in the positive ion mode at Q1 *m/z* 665.4 and Q3 *m/z* 445.3 for PP and at Q1 *m/z* 669.4 and Q3 *m/z* 449.3 for JNJ-3905343. The chromatographic and mass spectrometric conditions for the quantification of PAL and JNJ-17340362 were identical to those reported previously.(Darville et al. 2014)

PP, PAL and the internal standards were provided by Janssen Pharmaceutica NV (Beerse, Belgium). All solvents for sample preparation and chromatographic analysis were of liquid chromatography grade. The data acquisition and processing were performed using the Analyst® v1.5 software (Applied Biosystems Inc., Foster City, CA, USA).

SUPPLEMENTAL RESULTS

Temporal Evolution of the Local Inflammatory Response

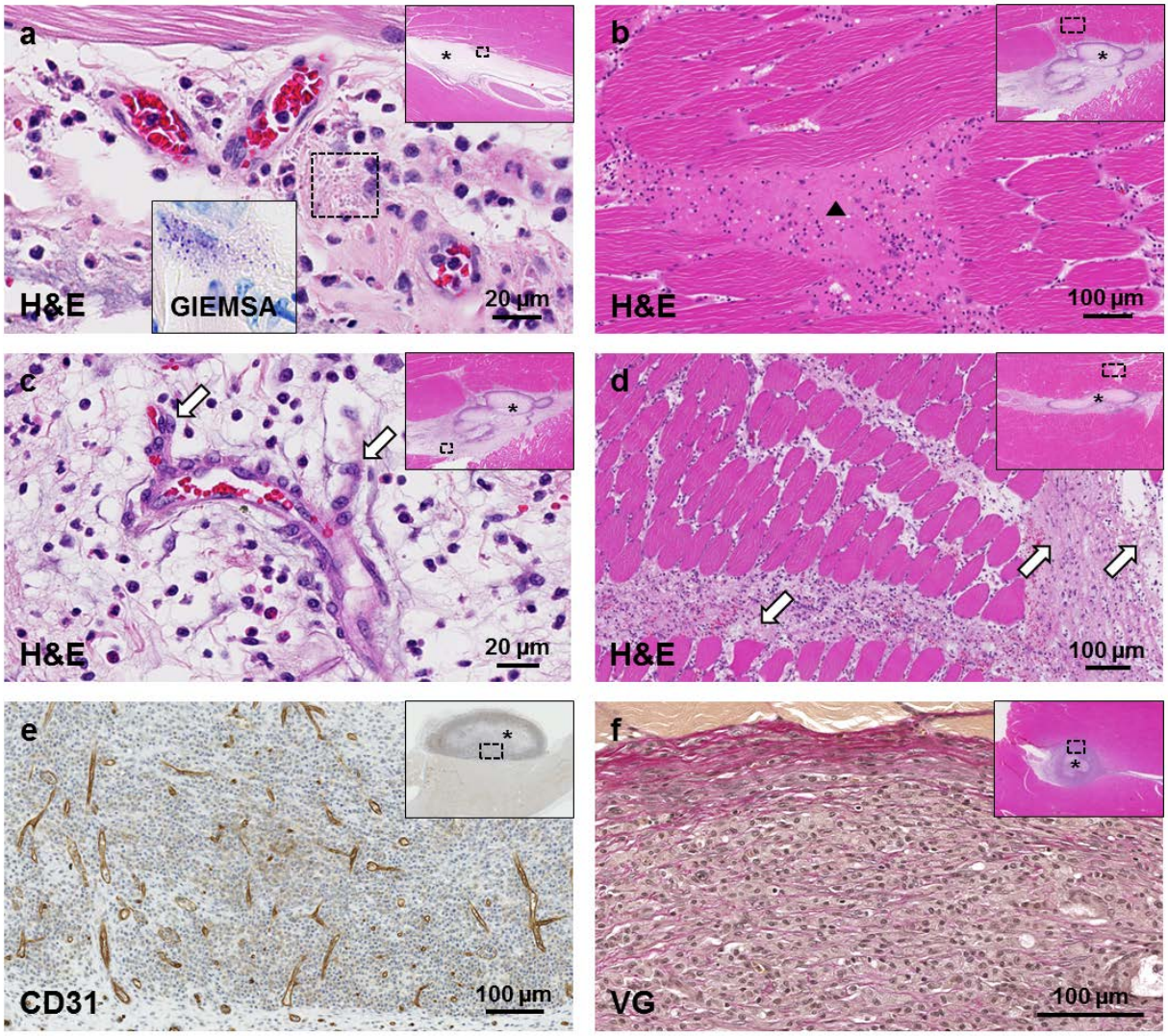

Figure S-2. Characteristic histopathological features of the inflammatory response according after a single im injection of PP-LAI or PS in the rat hind limb. (**a**) Degranulating perivascular mast cells (PP-LAI, 4 h). (**b**) Protein-rich eosinophilic oedema (▲) in endomysium (PP-LAI, 24 h). (**c**) Endothelial activation, hypertrophy and capillary sprouting (arrows) (PP-LAI, 24 h) (**d**) Interstitial fibrin deposition (arrows) (PP-LAI, 48 h). (**e**) Radial $CD31^{+}$ angiogenesis within the formulation depot (PP-LAI, 7 days). (**f**) Thin collagen deposition in outer portions of inflammatory capsule (PP-LAI, 14 days). The findings are representative of 3 animals per time point.

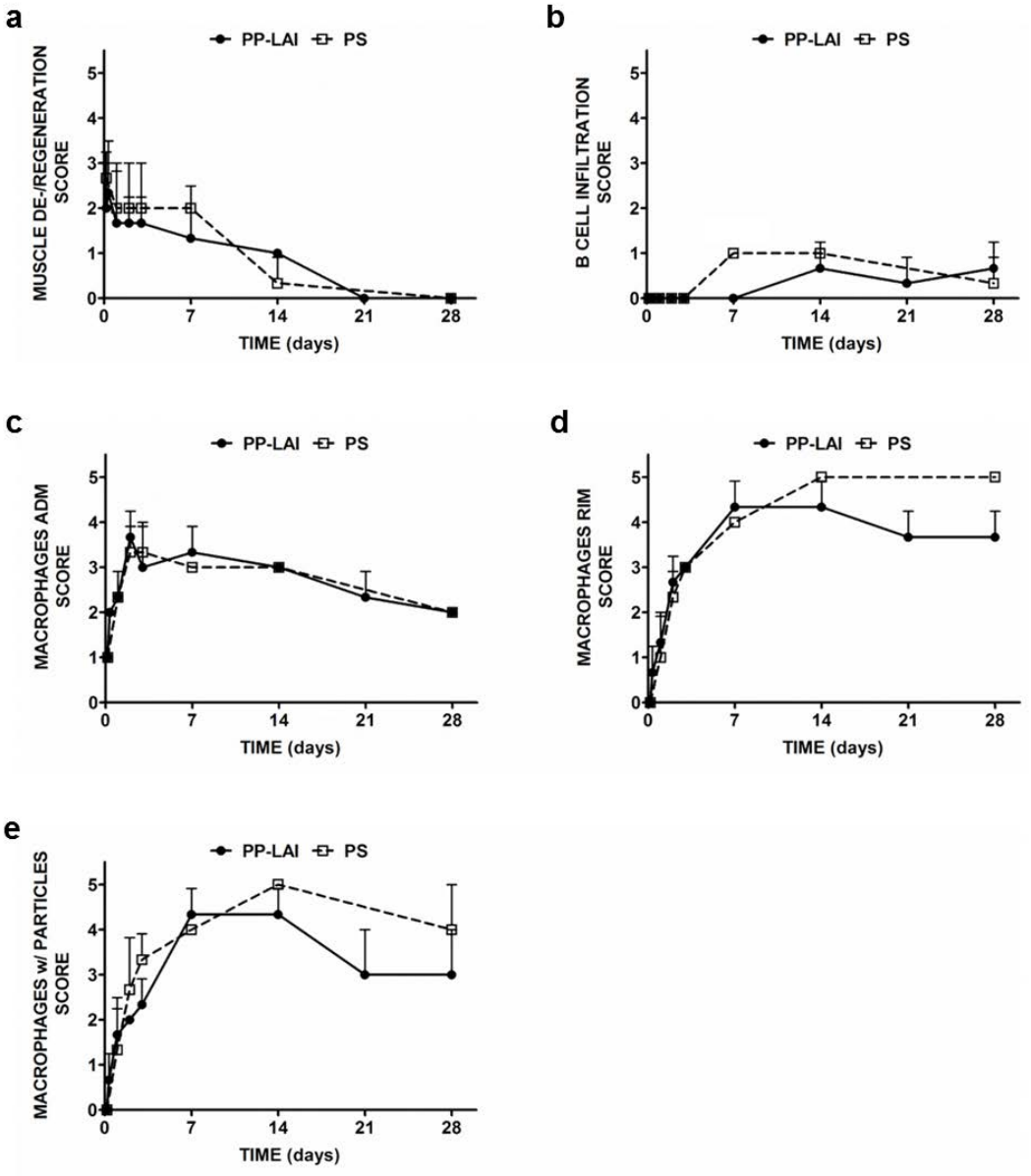

Figure S-3. Temporal evolution of histopathological parameters following a single im injection of PP-LAI (●) or PS (□) in the rat. Criteria for scoring are provided in the text. All parameters are expressed as mean scores on a semi-quantitative scale (0–5) ± SD (n = 3).

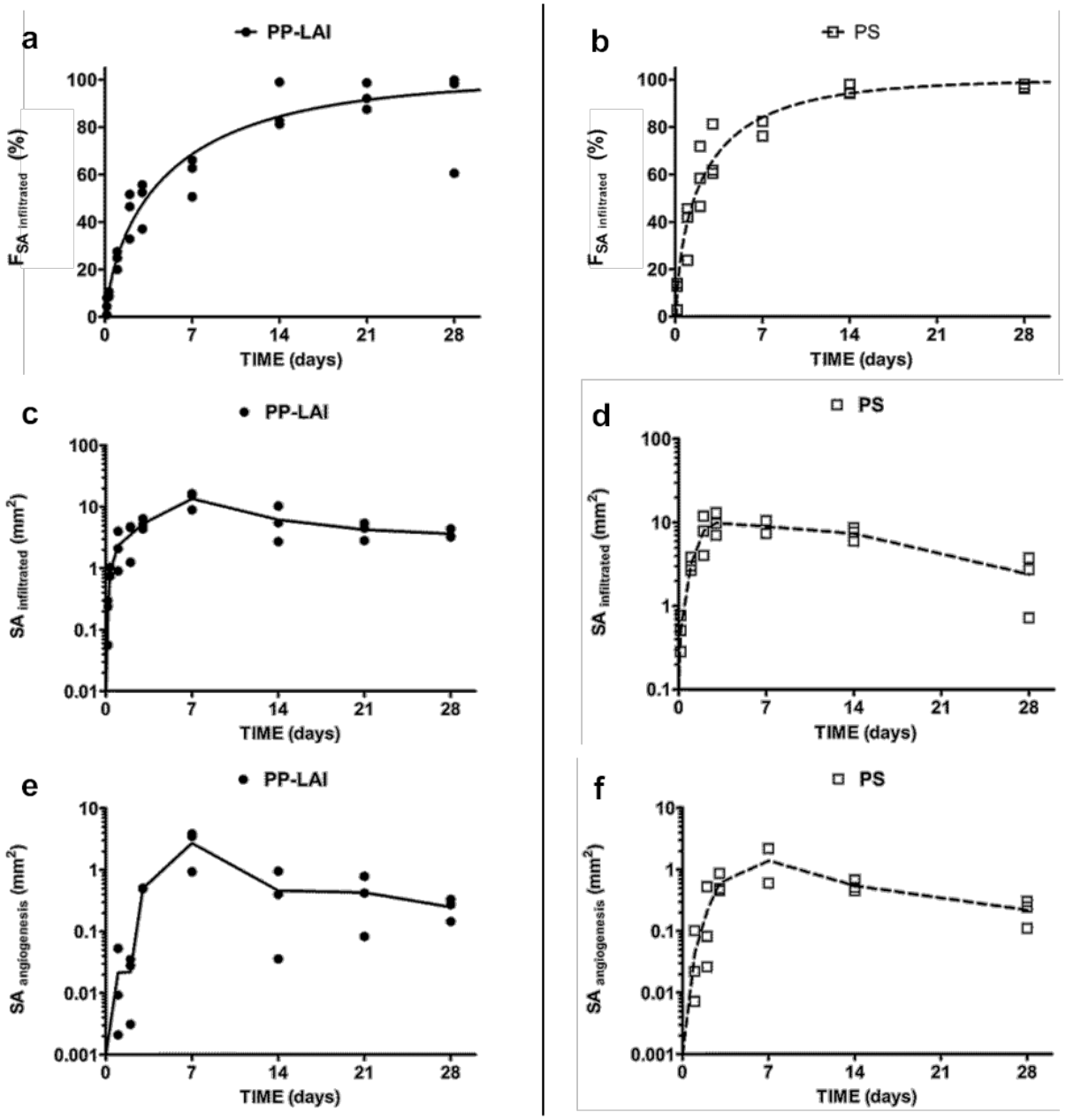

Figure S-4. Quantitative characterization of the PP-LAI (●) and PS (□) depot dimensions and cellularization as a function of time after a single im administration in the rat. (**a–b**) Measured individual (data points) and mean (lines) absolute cross-sectional areas of the formulation depots being infiltrated by inflammatory cells. (**c–d**) Calculated fractions of the cross-sectional area of the formulation depots being infiltrated by inflammatory cells (data points) and best fits of the 3-parameter cumulative Weibull distribution (lines). The open circle was identified as an outlier using ROUT's method and was excluded for regression analysis and subsequent volume calculations. (**e–f**) Measured individual (data points) and mean (lines) absolute cross-sectional areas of the $CD31^+$ vessels vascularizing the formulation depots.

Table S-2. Determination coefficients and model parameters of the modified cumulative 3-parameter Weibull distribution model obtained through nonlinear regression for the fraction of cross-sectional depot area infiltrated ($F_{S,infiltr.}$).[a,b]

	PP-LAI		PS***	
Model coefficients	Mean ± SE	95% CI	Mean ± SE	95% CI
R^2	0.9574	-	0.9414	-
α (days)	3.184 ± 0.411	2.332 – 4.035	1.807 ± 0.236**	1.310 – 2.305
β	0.676 ± 0.065	0.541 – 0.811	0.621 ± 0.100	0.411 – 0.832
T_0 (days)	0.115 ± 0.085	0.000 – 0.289	0.103 ± 0.072	0.000 – 0.254
$T_{50\%}$ (days)	3.341 ± 0.265	2.706 – 3.976	1.540 ± 0.059	1.098 – 1.982

[a] α, β and T_0, primary model parameters; $T_{50\%}$ secondary model parameter.

[b] Measured from histological sections through quantitative image analysis.

[c] Calculated from the fractional area infiltrated.

* Statistically significant difference between PP-LAI and PS, with *$p < 0.05$, **$p < 0.01$ and ***$p < 0.001$.